Figures and Legends

Fig. 1

Bombyx mori and their pheromone components

A: A male *B. mori*.

B: Pheromone of *B. mori* consists of two components, bombykol (major component) and bombykal (minor component).

A

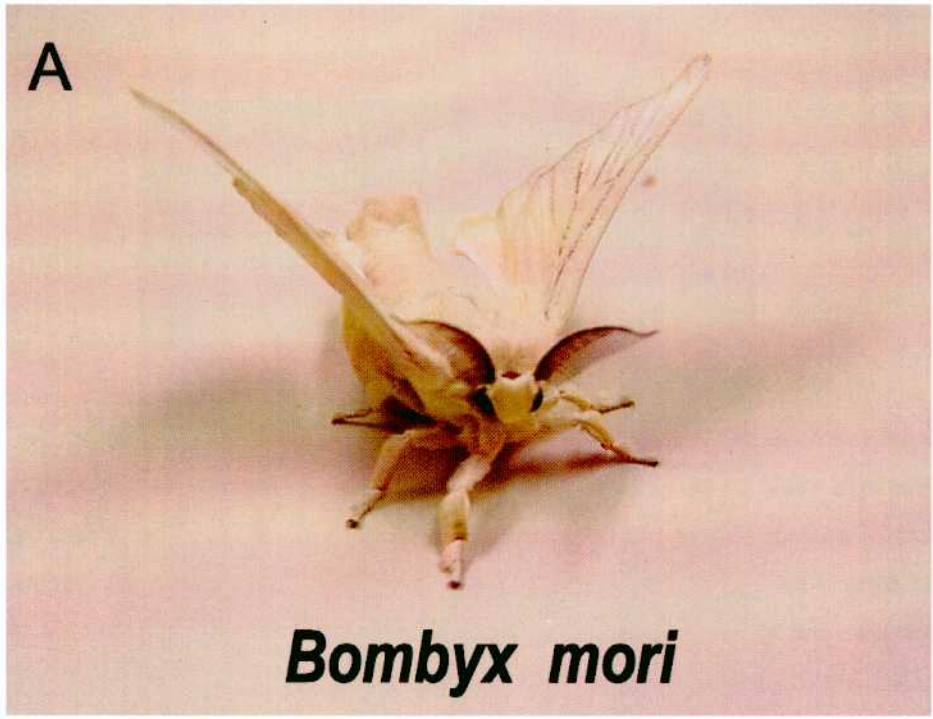

B

bombykol, (E,Z)-10,12-Hexadecadien-1-ol

bombykal, (E,Z)-10,12-Hexadecadienal

Fig. 2

Intracellular staining under visual control with a DIC microscope

A: Stereoscopic view of an isolated brain held by two supporting glass electrodes on the optic lobes. The box shows the region magnified in B, C. **B, C**: The lateral cell cluster of the antennal lobe visualized with a DIC microscope. The electrode (arrow in B) is filled with LY. The target cell body (arrow head in B) is impaled and then LY is injected to it (C) (see Materials and Methods).

Scale bars = 1 mm in A, 50 μm in B, C

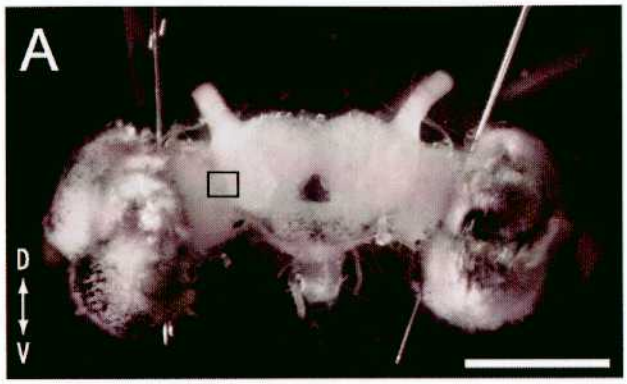
A
D
V

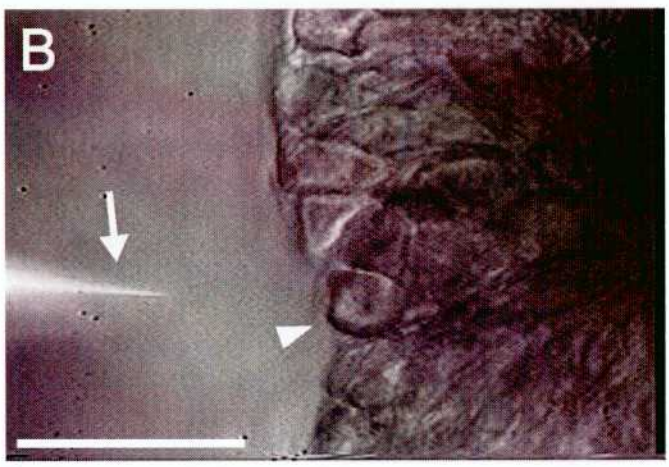
B

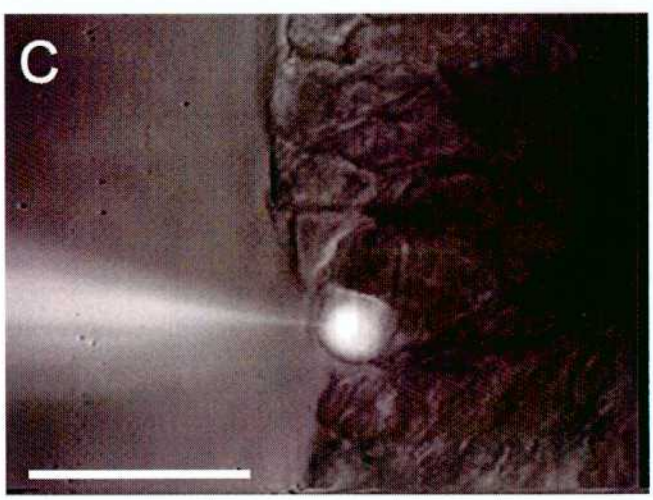
C

Fig. 3

Infrared DIC microscopic system

Cell bodies are visualized with a fixed-stage upright microscope equipped with DIC optics and long-working distance objectives (x40 LUMPlanFL/IR or x60 LUMPlanFL/IR water immersion). Infrared transmitted beam (including wavelength over 750nm) lights the preparation on the stage. DIC effect is made by the DIC elements (polarizer, analyzer, DIC prisms). A CCD camera controller enhances contrast. The microscope attaches fluorescent optics. The amplifier is used for current injection of the fluorescent dye. (see Materials and Methods)

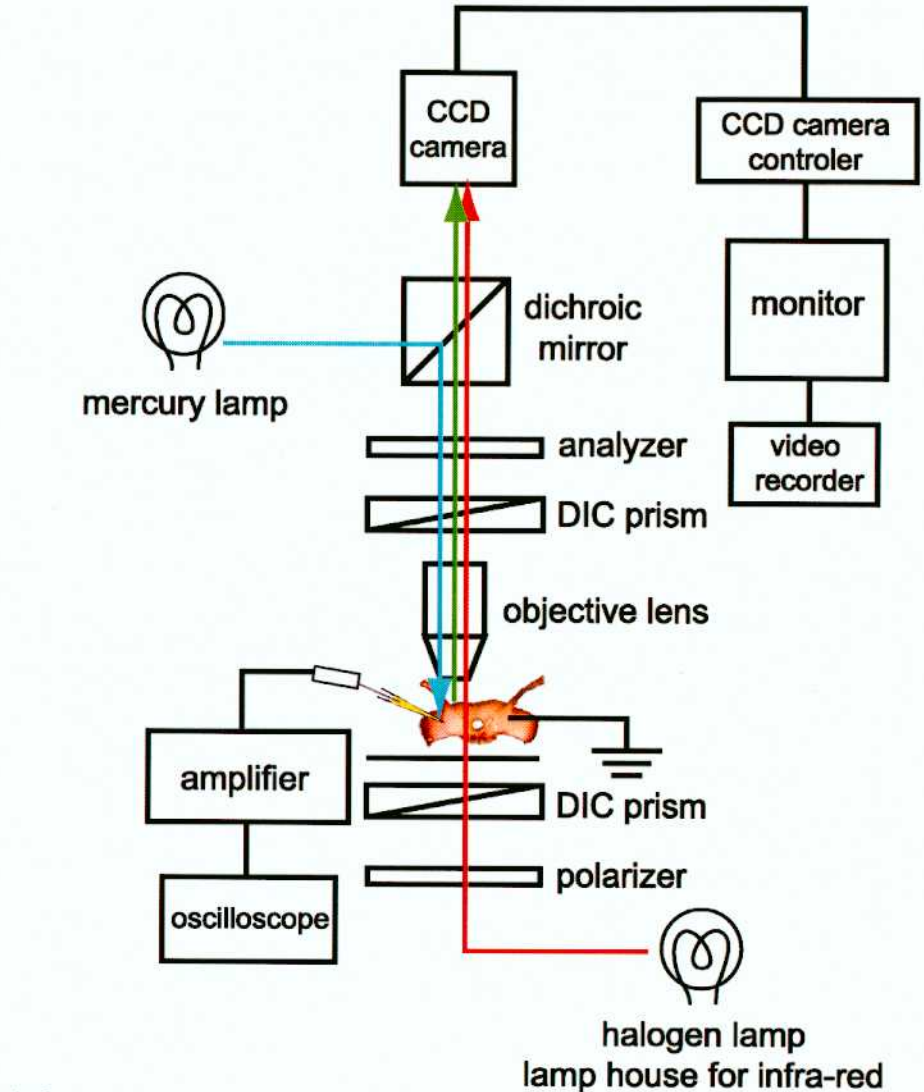

infrared transmitted beam

fluorescent excitation light

emission light

Fig. 4

NO/cGMP cascade

NO is free radical working intra and intracellularly. NO is synthesized by NO synthase (NOS) from L-arginine and O_2 with L-citrulline. NOS is activated by Ca- Calmodulin. NO diffuse three dimensionally and activate soluble guanylyl cyclase (sGC) in target neurons. sGC synthesize cyclic guanosine monophosphate (cGMP). For anti-cGMP immunostaining the brains were preincubated in 1mM 3-isobutyl-1-methyxanthine (IBMX) to block endogenous phosphodiesterase (PDE) activity. Soluble guanylyl cyclase was stimulated by a NO donor, 10 mM sodium nitroprusside (SNP) or 200 mM S-nitroso-N-acetylpenicillamine (SNAP).

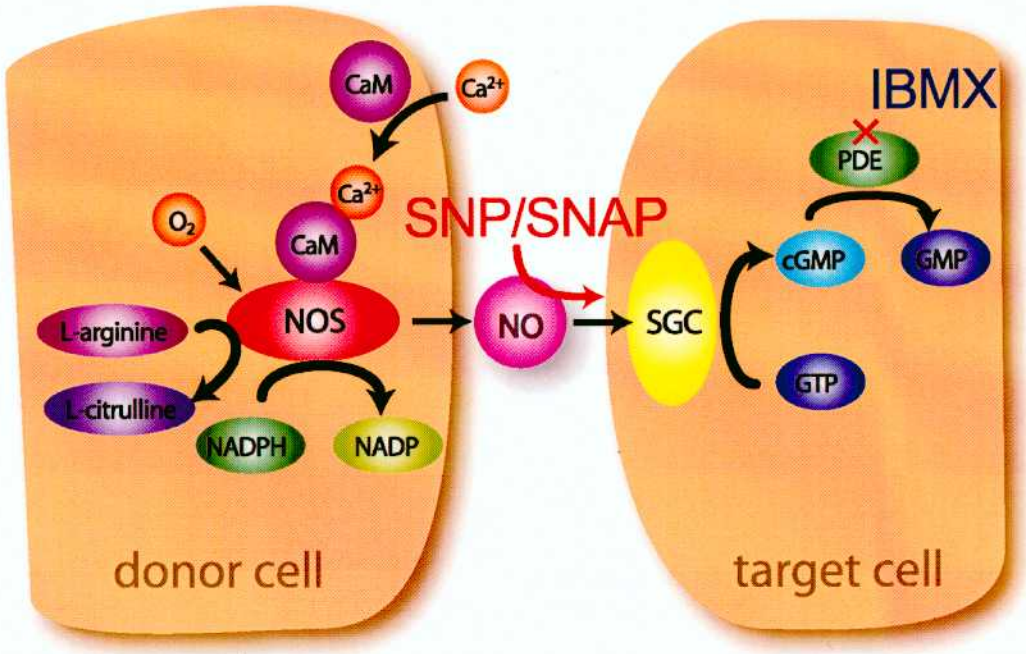
CaM
Ca2+
Ca2+
CaM
O2
SNP/SNAP
L-arginine
NOS
NO
SGC
L-citrulline
NADPH
NADP
donor cell
target cell
IBMX
PDE
cGMP
GMP
GTP

Fig. 5

Anti-cGMP immunostaining is used for a structural marker in the LPC

A-D: Anti-cGMP immunostaining shows the specific deltoid region in the LPC. This deltoid region is observed in every individual consistently. A-D shows different individuals applied with anti-cGMP immunostaining. Frontal view. Scale bars = 100 μm.

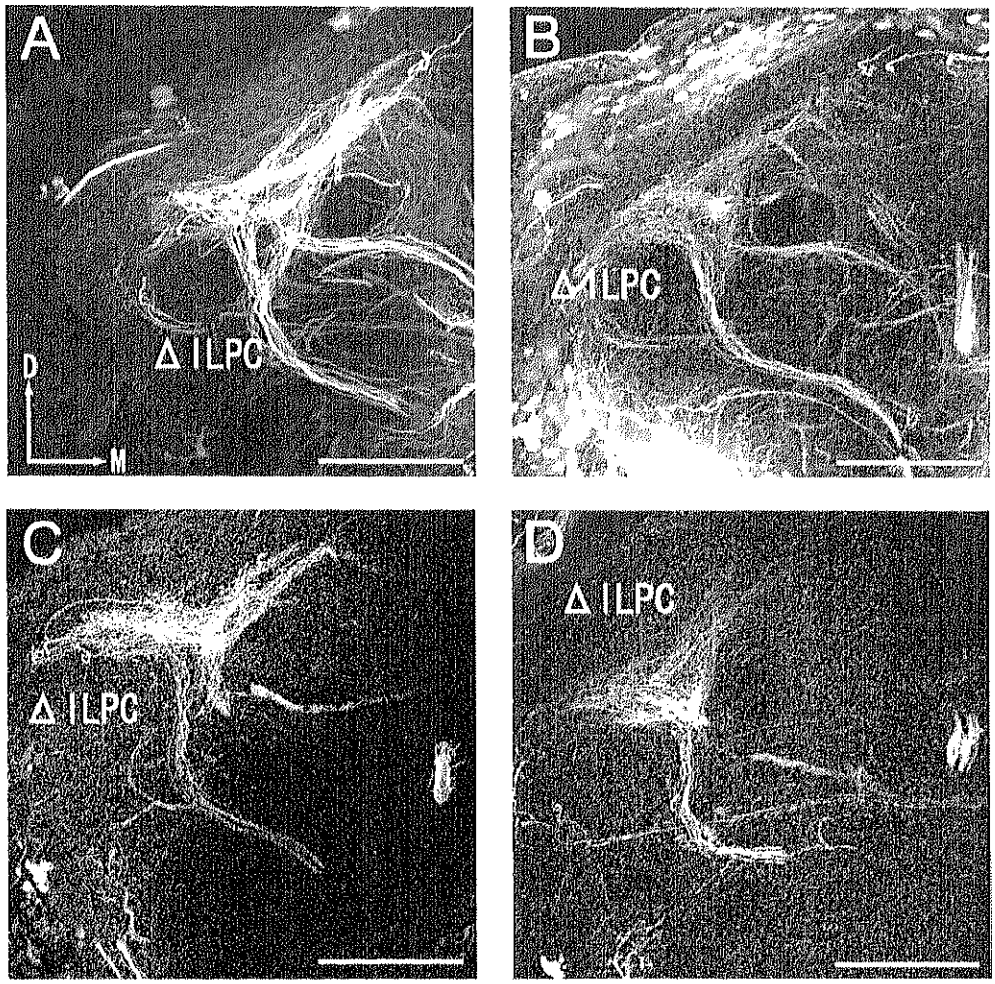
A
ΔILPC
D
M
B
ΔILPC
C
ΔILPC
D
ΔILPC

Fig. 6

Examples of neurons stained with the newly developed intracellular staining method

A-F show projection image of full structures of each neuron (upper) and schematic diagrams of each neuron showing the cell body position and the neural pathway to the whole brain (under).

A: An antennal lobe LN. **B**: An antennal lobe PN. **C**: A Kenyon cell. **D-F**: Descending neurons known as Group I (D), Group II (E) and Group III (F). These neurons are thought to play important roles in olfactory processing.

Scale bars = 100 μm.

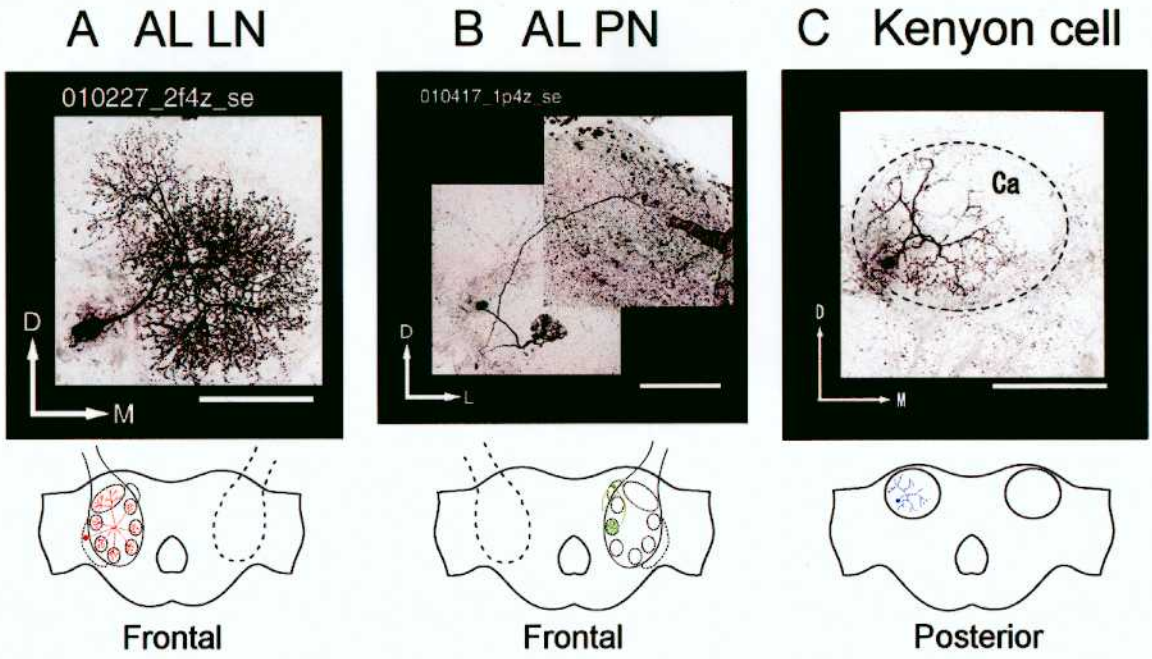
A AL LN
B AL PN
C Kenyon cell
010227_2f4z_se
010417_1p4z_se
Ca
D
M
L
Frontal
Frontal
Posterior

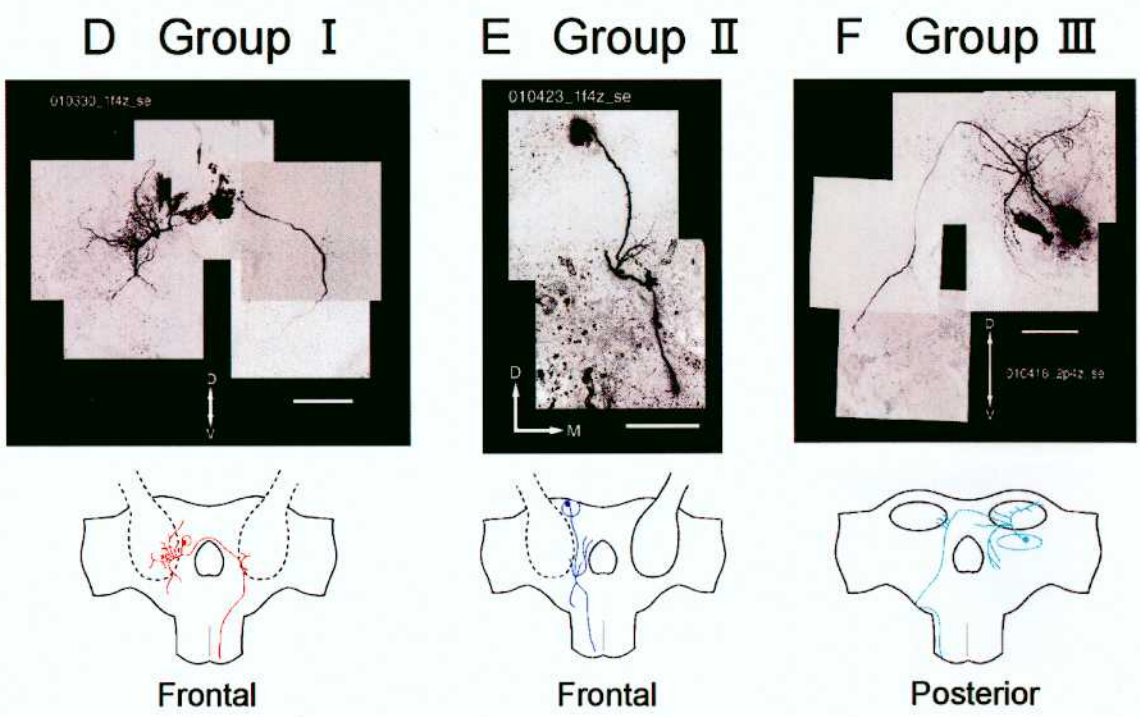
D Group I
E Group II
F Group III
010423_1f4z_se
D
M
V
Frontal
Frontal
Posterior

Fig. 7

Other examples of neurons stained with the newly developed intracellular staining method and schematic diagram of cell cluster positions of sampled neurons.

A-D show projection image of full structures of each neuron (upper; left in B) and schematic diagrams of each neuron showing the cell body position and the neural pathway to the whole brain (under; right in B).

A: A bilateral neuron in the protocerebrum. **B**: A neurosecretory cell. **C**: An efferent neuron to the optic lobe. **D**: An efferent neuron to the optic lobe.

These neurons are not known about their function. **E, F**: Schematic diagrams showing the cell clusters of stained neurons in this study. Frontal view (E) and posterior view (F). Scale bars = 100 μm.

A Bilateral neuron

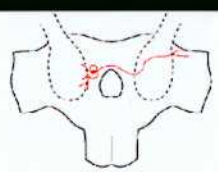

Frontal

B Neurosecretory cell

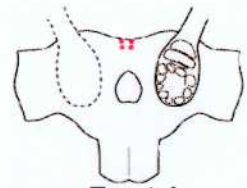

Frontal

C Optic efferent neuron 1

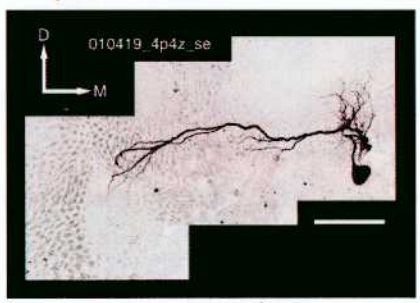

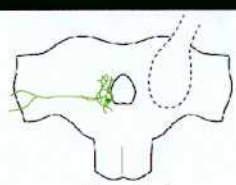

Frontal

D Optic efferent neuron 2

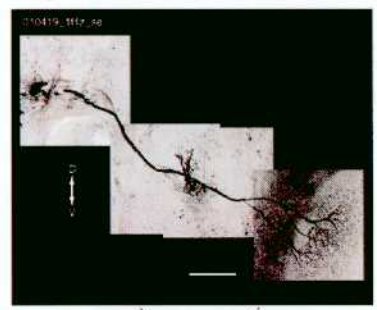

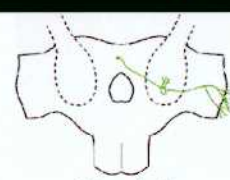

Frontal

E

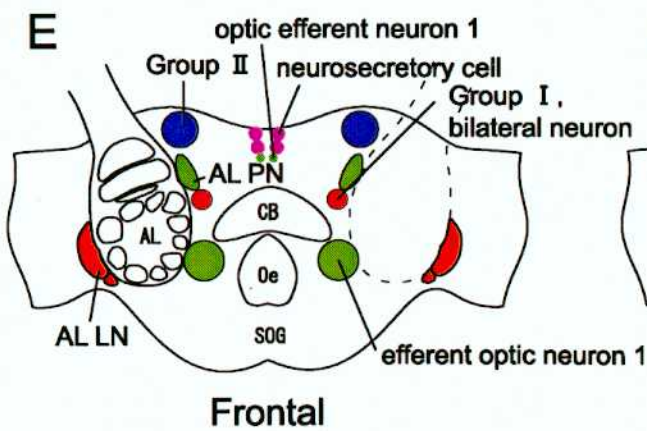

Frontal

F

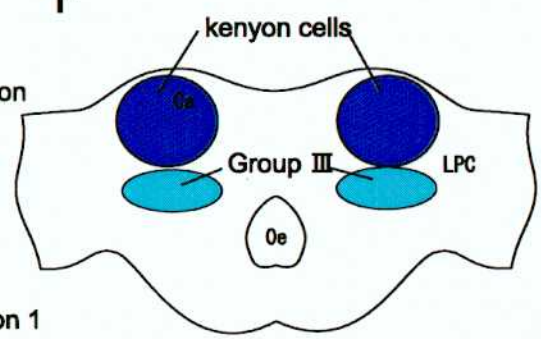

Posterior

Fig. 8

NO-induced anti-cGMP immunostaining in the protocerebrum and the AL of *B. mori*. Strong immunoreactivity is observed in the toroid of the MGC in the AL and the ΔILPC in the LPC. The ΔILPC becomes a landmark in the LPC. **A**: Projection image of NO-induced anti-cGMP immunostaining. Frontal view. The dashed line links processes that were separated to reveal the structures of branches that overlapped *in situ*. **B**: Projection image of NO-induced anti-cGMP immunostaining in the LPC. The ΔILPC is observed within the triangle outline. Frontal view. **C**: Schematic drawing of a hemisphere of the brain showing NO-induced anti-cGMP immunoreactive pathways from the dorsal view. **D, E**: 3-D reconstructions of the cGMP immunostaining in the LPC from the front-dorsal view (D) and dorsal view (E). The MB is outlined with a transparent color showing its relative position in the LPC. **F, G**: Confocal slice images of NO-induced anti-cGMP immunostaining in the AL. These two images clearly show toroid specific arborizations in the MGC. The toroid shows specifically stronger immunoreactivity than the cumulus and other areas in the MGC. Frontal view. **H**: Projection image of NO-induced anti-cGMP immunostaining in the AL. Tracing the OACT leads to the MGC (black arrow). They have cell bodies in the LC and exit the AL through the OACT (dashed black arrow). Frontal view. Scale bars = 100 μm.

AL, antennal lobe; Ca, calyx of the mushroom body; ΔILPC, delta area in the inferior lateral protocerebrum; G, ordinary glomerulus; Gs, ordinary glomeruli; IACT, inner antenno-cerebral tract; LC, lateral cell cluster of the AL; MACT middle antenno-cerebral tract; MC, medial cell cluster of the AL; MGC, macroglomerular complex; OACT, outer antenno-cerebral tract

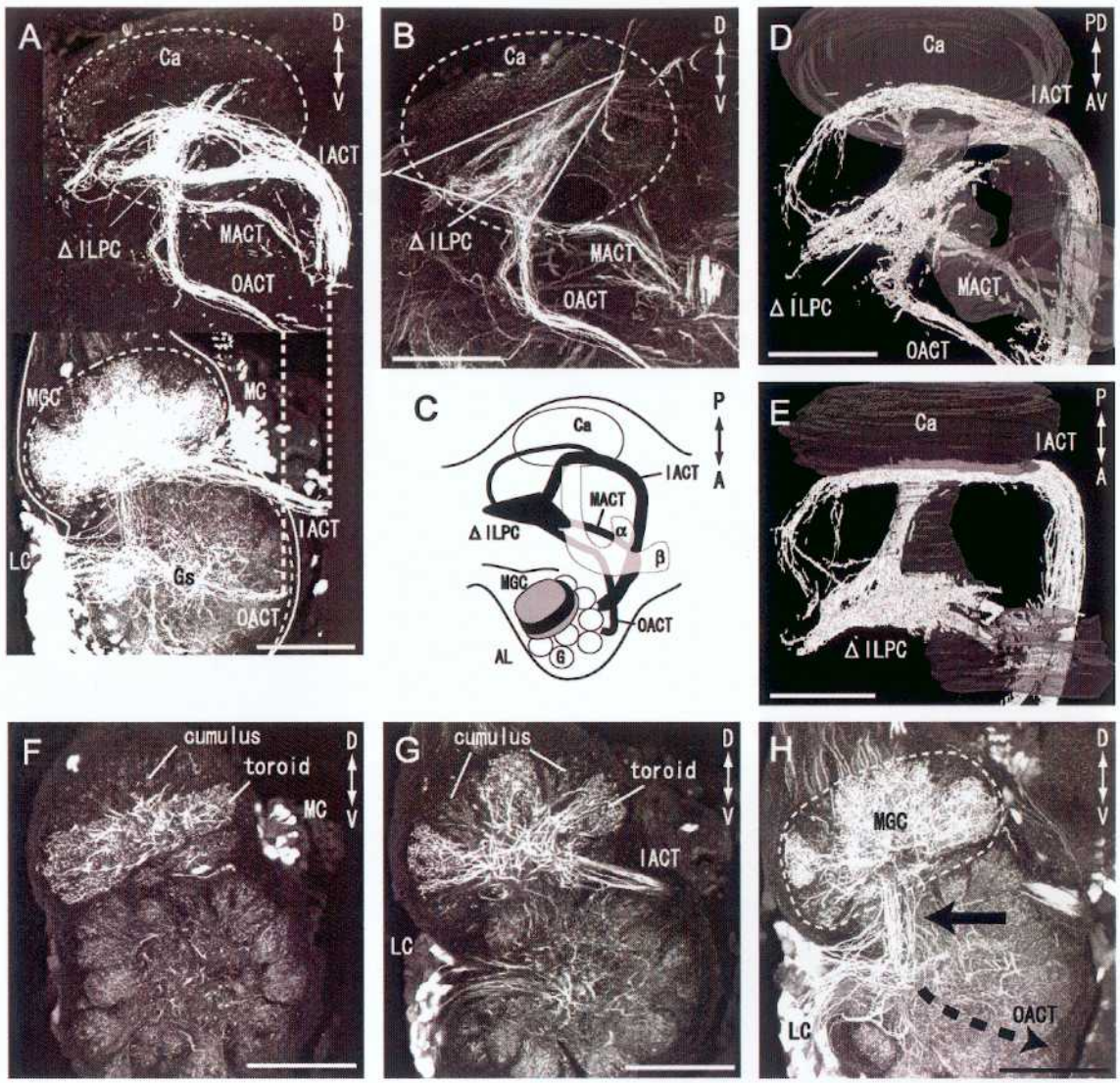
A
Ca
D
V
lACT
ΔlLPC
MACT
OACT
MGC
MC
LC
Gs
B
C
P
A
α
β
AL
G
D
PD
AV
E
F
cumulus
toroid
G
H

Fig. 9

Toroid-PN. **A**: Full structure of a toroid-PN. Dendritic arborizations are restricted to the toroid of the MGC. The cell body is in the MC. The axon runs in the IACT and sends a few short branches to the Ca and blebby branches to the LPC. Frontal view. The dashed line links processes that were separated to reveal the structures of branches that overlapped *in situ*. **B**: 3-D reconstruction of the projection pattern of the toroid-PN to the LPC from the front-dorsal view. Arrow indicates a few short branches in the Ca. **C**: Schematic drawing of a hemisphere of the brain showing morphology of the toroid-PN from the dorsal view. **D**: Axonal projections in the LPC of the toroid-PN (colored yellow; note that LY staining green color is overlapped with cGMP's red color) with NO-induced anti-cGMP immunostaining (colored red). Frontal view. **E**: Dendritic arborizations in the AL of the toroid-PN (colored yellow; note that LY staining green color is overlapped with cGMP's red color) with NO-induced anti-cGMP immunostaining (colored red). Frontal view. **F, G**: 3-D reconstructions of the toroid-PN (colored green) and cGMP immunoreactive neurons (colored red) in the LPC from the frontal view (F) and dorsal view (G). The MB is outlined transparently. Scale bars = 100 μm.

AL, antennal lobe; Ca, calyx of the mushroom body; ΔILPC, delta area in the inferior lateral protocerebrum; G, ordinary glomerulus; Gs, ordinary glomeruli; IACT, inner antenno-cerebral tract; MC, medial cell cluster of the AL; MGC, macroglomerular complex

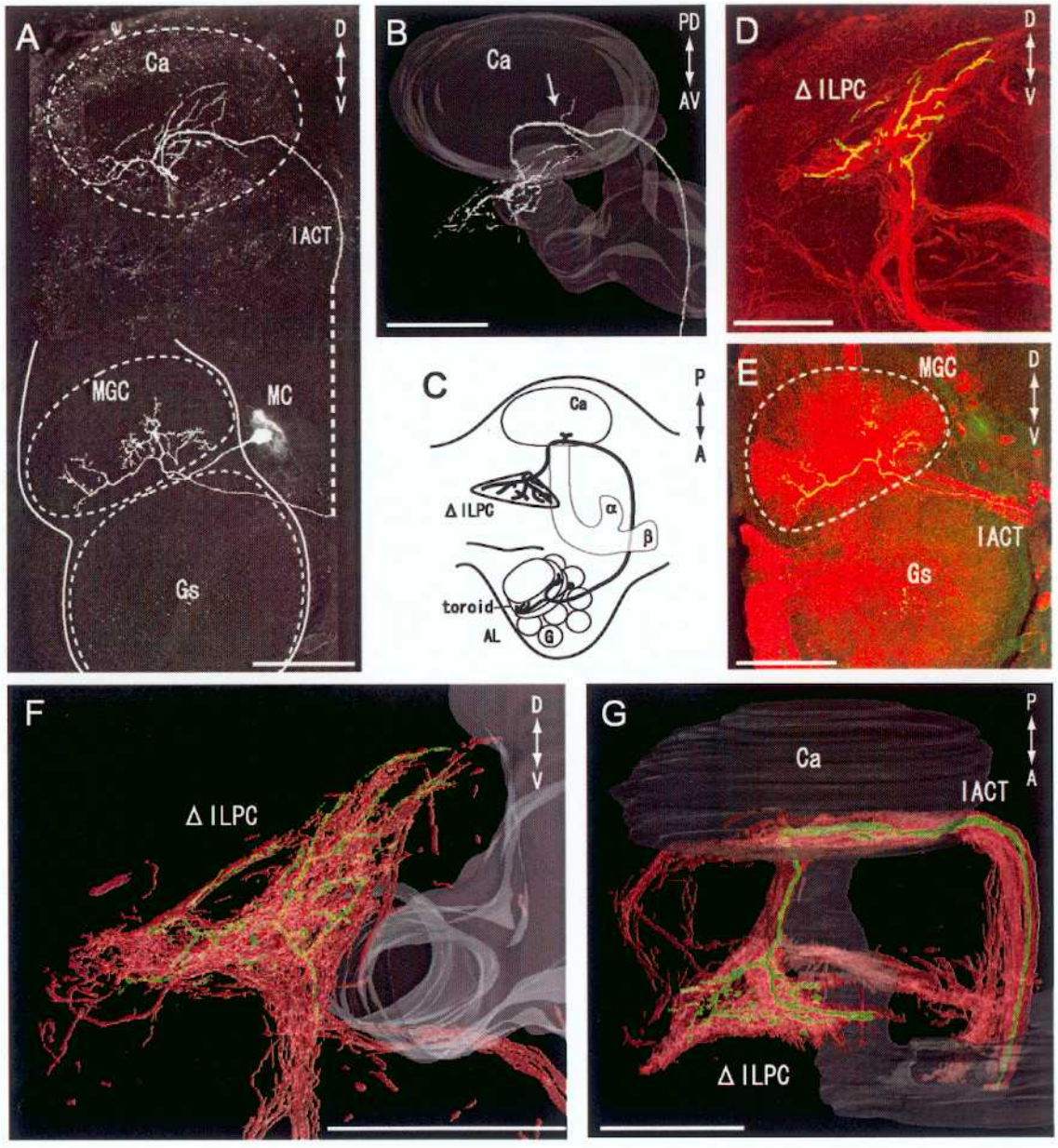
A
Ca
D
V
lACT
MGC
MC
Gs
B
Ca
PD
AV
C
Ca
P
A
ΔlLPC
α
β
toroid
AL
θ
D
ΔlLPC
V
E
MGC
D
V
lACT
Gs
F
D
ΔlLPC
V
G
Ca
P
A
lACT
ΔlLPC

Fig. 10

Cumulus -PN. **A**: Full structure of a cumulus-PN. Dendritic arborizations are restricted to the cumulus of the MGC. The cell body is in the MC. The axon runs in the IACT and sends blebby branches to the Ca and the LPC. Frontal view. The dashed line links processes that were separated to reveal the structures of branches that overlapped *in situ*. **B**: 3-D reconstruction of the projection pattern of the cumulus-PN to the LPC from the front-dorsal view. **C**: Schematic drawing of a hemisphere of the brain showing morphology of the cumulus-PN from the dorsal view. **D**: Axonal projections in the LPC of the cumulus-PN (colored green) with NO-induced anti-cGMP immunostaining (colored red). Frontal view. **E**: Dendritic arborizations in the AL of the cumulus-PN (colored green) with NO-induced anti-cGMP immunostaining (colored red). Frontal view. **F, G**: 3-D reconstructions of the cumulus-PN (colored green) and cGMP immunoreactive neurons (colored red) in the LPC from the frontal view (F) and dorsal view (G). The MB is outlined transparently. Scale bars = 100 μm.

AL, antennal lobe; Ca, calyx of the mushroom body; ΔILPC, delta area in the inferior lateral protocerebrum; G, ordinary glomerulus; Gs, ordinary glomeruli; IACT, inner antenno-cerebral tract; MC, medial cell cluster of the AL; MGC, macroglomerular complex

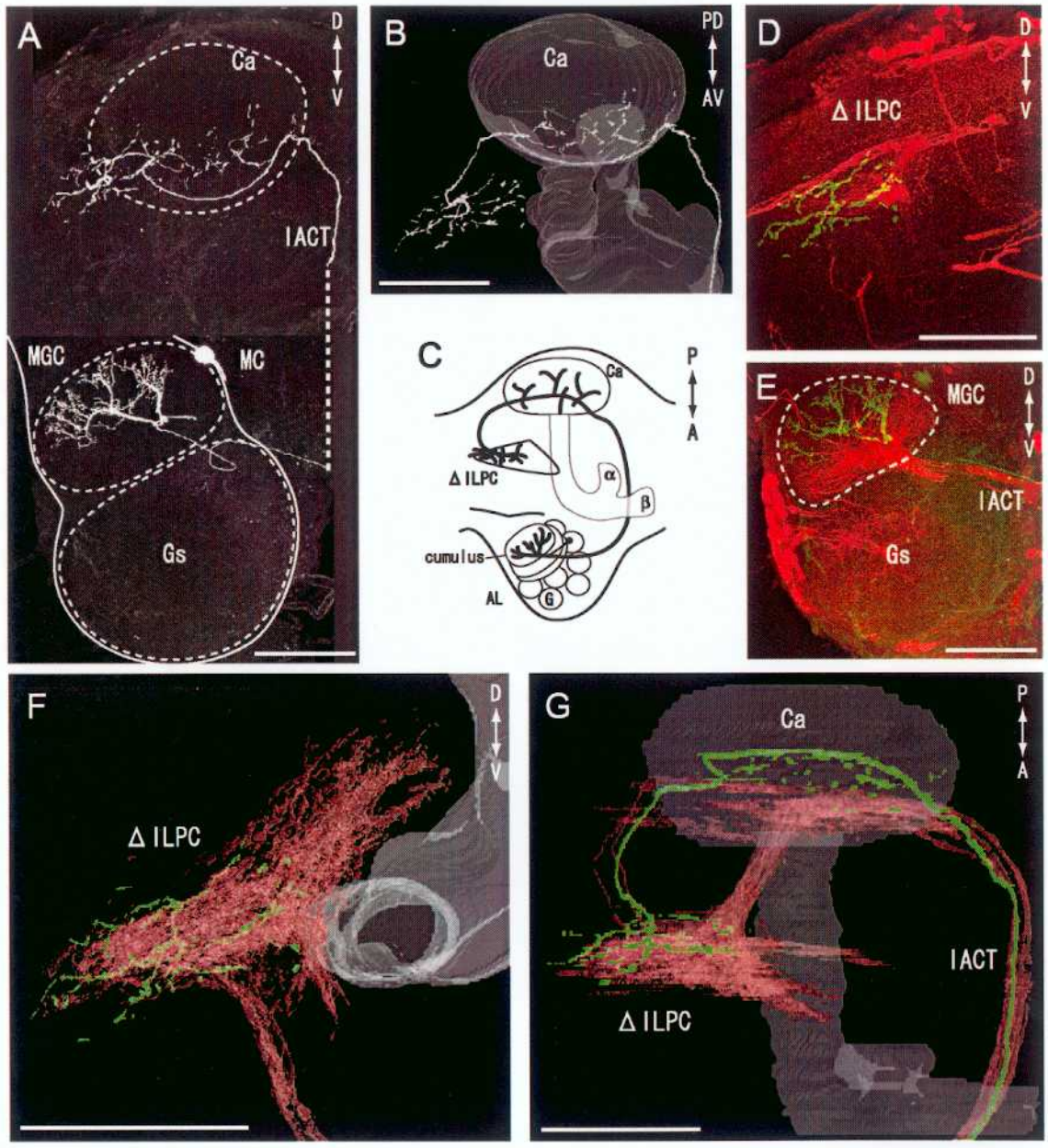
A
D
V
Ca
lACT
MGC
MC
Gs
B
PD
AV
Ca
C
P
A
Ca
Δ ILPC
α
β
cumulus
AL
G
D
D
V
Δ ILPC
E
MGC
D
V
lACT
Gs
F
D
V
Δ ILPC
G
Ca
P
A
lACT
Δ ILPC

Fig. 11

Horseshoe-PN. This data was obtained from a sectioned brain preparation. **A**: Axonal projections in the LPC of the horseshoe-PN (colored green) with NO-induced anti-cGMP immunostaining (colored red). Frontal view. **B**: Dendritic arborizations in the AL of the horseshoe-PN (colored green) with NO-induced anti-cGMP immunostaining (colored red). Frontal view. **C**: Schematic drawing of a hemisphere of the brain showing morphology of the horseshoe-PN from the dorsal view. Dendritic arborizations are restricted to the horseshoe of the MGC. The cell body is in the MC. The axon runs in the lACT and sends blebby branches to the Ca and the LPC. **D, E**: 3-D reconstructions of the horseshoe-PN (colored green) and cGMP immunoreactive neurons (colored red) in the LPC from the dorsal view (D) and frontal view (E). Scale bars = 100 μm.

AL, antennal lobe; Ca, calyx of the mushroom body; ΔILPC, delta area in the inferior lateral protocerebrum; G, ordinary glomerulus; Gs, ordinary glomeruli; MGC, macroglomerular complex

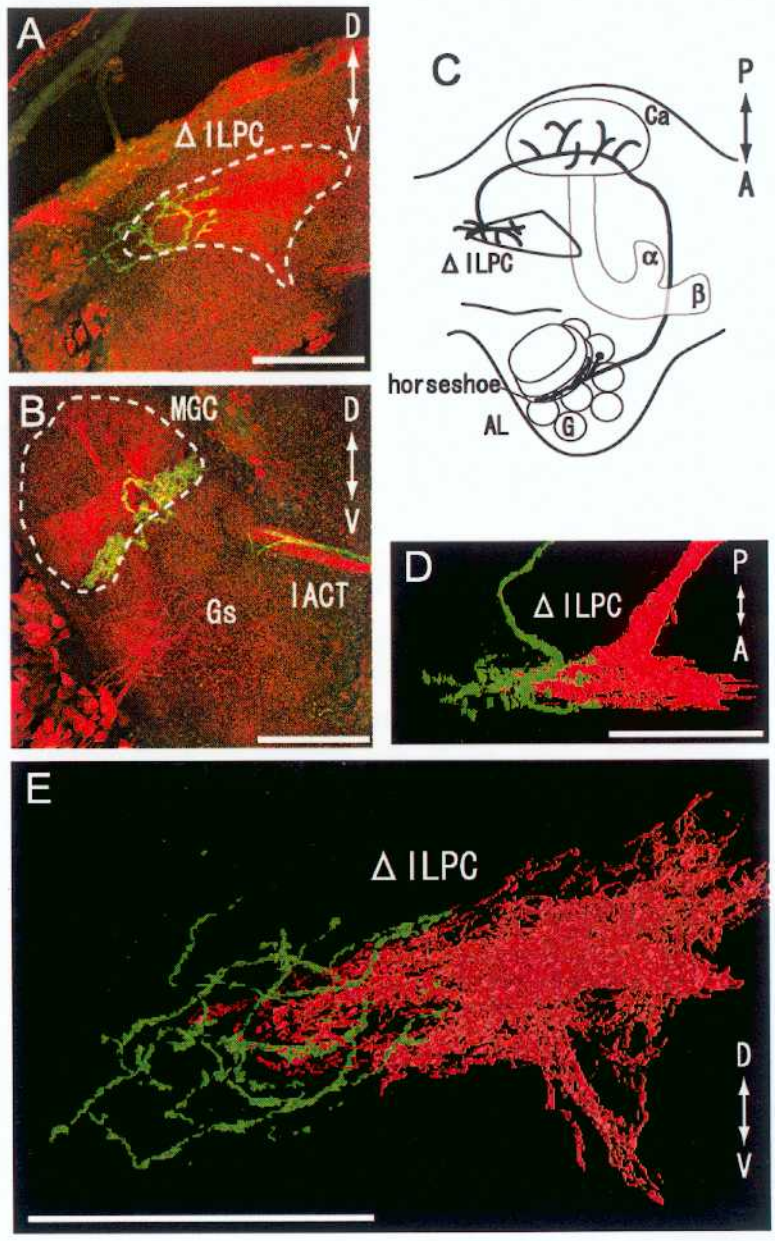
A
D
V
Δ ILPC
B
MGC
D
V
Gs
l ACT
C
P
A
Ca
Δ ILPC
α
β
horseshoe
AL
G
D
P
A
Δ ILPC
E
Δ ILPC
D
V

Fig. 12

G-PN. **A**: Full structure of a G-PN. Dendritic arborizations are restricted to two ordinary glomeruli of the AL. These two glomeruli are identifiable (Terada et al., 2003). The cell body is in the MC. The axon runs in the IACT and sends blebby branches to the Ca and the LPC. Frontal view. The dashed line links processes that were separated to reveal the structures of branches that overlapped *in situ*. **B**: 3-D reconstruction of the projection pattern of the G-PN to the LPC from the front-dorsal view. **C**: Schematic drawing of a hemisphere of the brain showing morphology of the G-PN from the dorsal view. **D**: Dendritic arborizations in the AL of the G-PN (colored green) with NO-induced anti-cGMP immunostaining (colored red). Frontal view. **E, F**: 3-D reconstructions of the G-PN (colored green) and cGMP immunoreactive neurons (colored red) in the LPC from the frontal view (E) and dorsal view (F). The MB is outlined transparently. Scale bars = 100 μm.

AL, antennal lobe; Ca, calyx of the mushroom body; ΔILPC, delta area in the inferior lateral protocerebrum; G, ordinary glomerulus; Gs, ordinary glomeruli; IACT, inner antenno-cerebral tract; LH, lateral horn; MC, medial cell cluster of the AL; MGC, macroglomerular complex

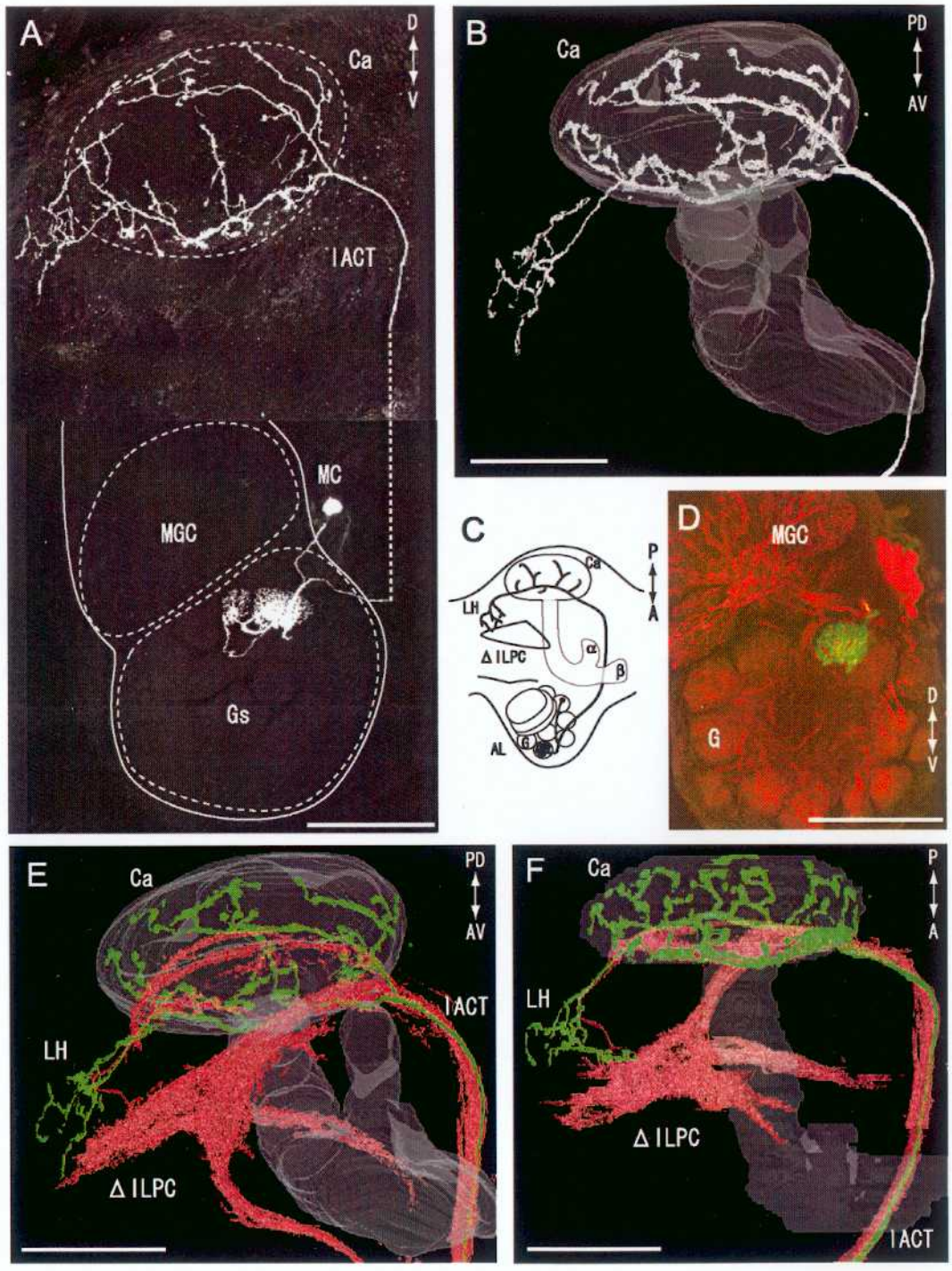
A
D
V
Ca
lACT
MC
MGC
Gs
B
Ca
PD
AV
C
Ca
P
A
LH
Δ ILPC
α
β
AL
G
D
MGC
G
D
V
E
Ca
PD
AV
lACT
LH
Δ ILPC
F
Ca
P
A
LH
Δ ILPC
lACT

Fig. 13

Divisions of the AL.

A-D: Confocal slice images of the antennal lobe stained with LY. The optical section is 0.75 μm. A-D are at the depth of 32, 81, 120, 134 μm respectively from anterior to posterior. Arrow in B shows the major tract from the LCI. Arrow in D shows the second thin tract from the LCII.

Scale bars = 100 μm in A-D.

C, cumulus; Gs, ordinary glomeruli; H, horseshoe; LC, lateral cell cluster of the AL; LLG1, lateral large glomerulus 1; LLG2, lateral large glomerulus 2 MC, medial cell cluster of the AL; MSG, medial small glomeruli; PV, posterior ventral region of the AL; T toroid

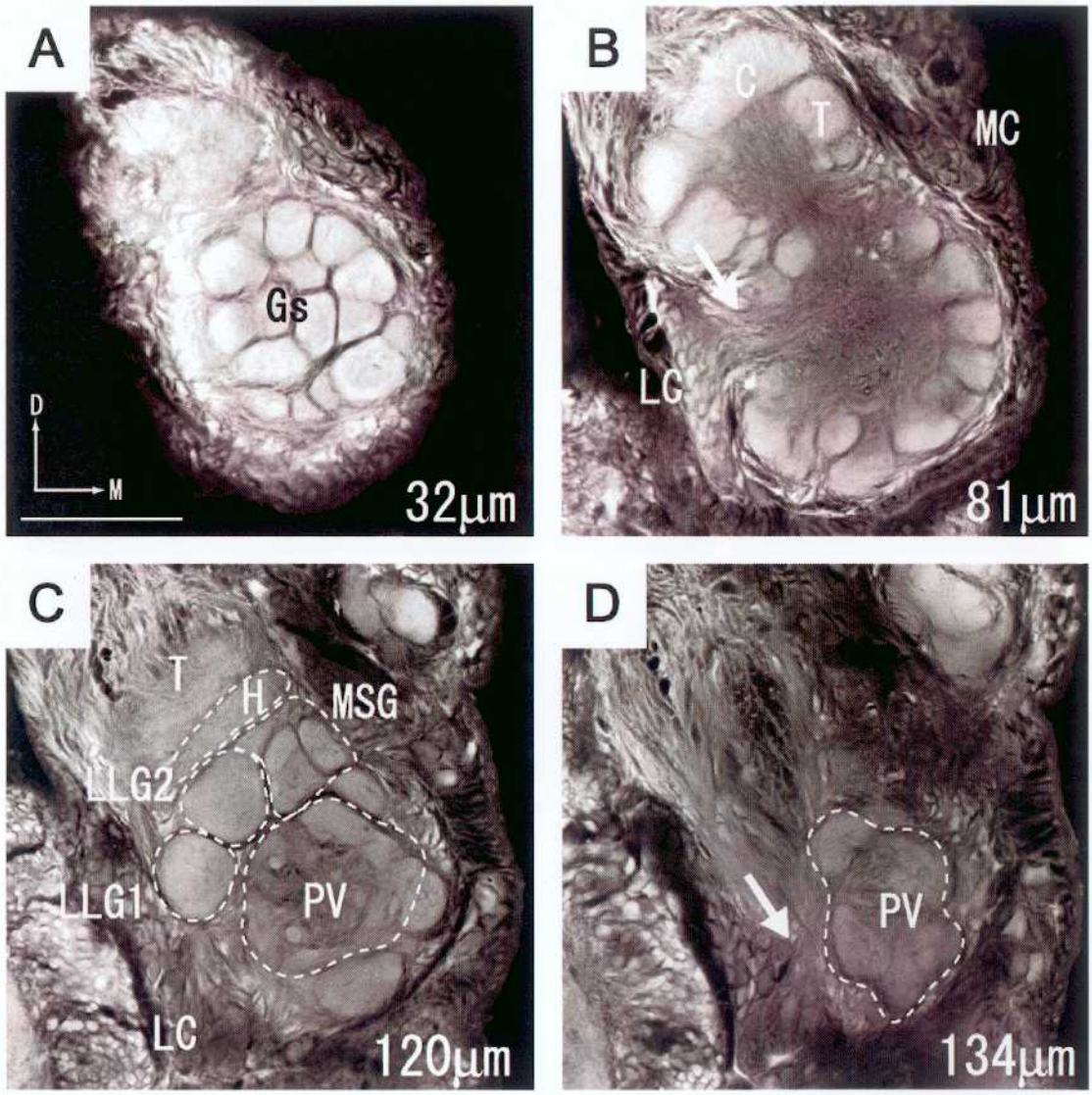
A
Gs
D
M
32μm
B
C
T
MC
LC
81μm
C
T
H
MSG
LLG2
LLG1
PV
LC
120μm
D
PV
134μm

Fig. 14

Type I LNs.

A: Full structure of the Type I LN. It arborizes in the MGC and almost all Gs. It has cell body in the LC I. It sends its main neurite to the center core of the AL and then radially branches. **B, C**: Another two examples of full structure of the Type I LN. In B the LN first bifurcates at the entrance of the AL (arrow). In C the LN has small arborization in the MGC. **D**: Projection image of several slices in the AL showing the dendritic distribution within a glomerulus. Coarse arborization biased to the core of a glomerulus is observed. The dashed line demarcates single glomerulus. **E**: Magnification view of dendritic branches. Branching studded with spine-like process are observed. **F**: Projection image of several slices in the MGC. It has sparse arborization in the MGC. No compartmental branching pattern is observed in each subdivision of the MGC.

Thickness of projection: D, 7.2 μm; E, 8 μm; F, 5.7 μm.

Scale bars = 100 μm in A-D, F; 20 μm in E.

C, cumulus; Cb, cell body; Gs, ordinary glomeruli; T toroid

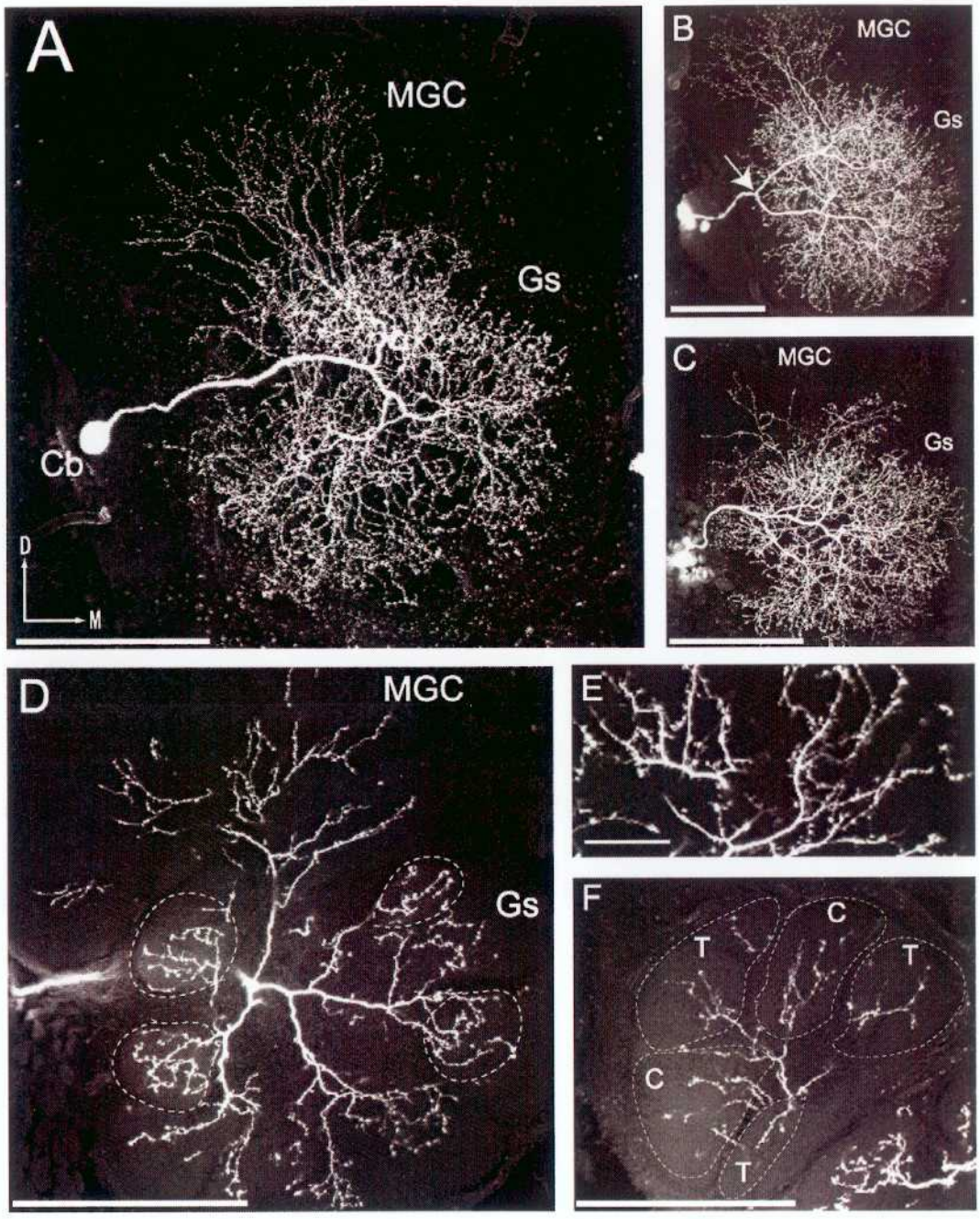
A
MGC
Gs
Cb
D
M
B
MGC
Gs
C
MGC
Gs
D
MGC
Gs
E
F
C
T
T
C
T

Fig. 15

Type II LNs.

A: Full structure of the Type II LN. It arborizes in the MGC and almost all Gs. It has cell body in the LC II. It sends its main neurite through the under thin tract to the posterior region to central core of the AL. **B**: Projection image of a few slices in the MGC. It arborizes sparsely in the MGC. Central fiber core region of the MGC is densely arborized. Arborization in the toroid is notably fewer. C: Projection image of a few slices showing the bifurcation of the main neurite at the posterior to the central fiber core. **D**: Projection image of a few slices showing dense arborization in the PV and sparse arborization in the LLG1,2 and MSG. **E**: Projection image of a few slices in the anterior side of Gs. Note that dense arborization is observed within the Gs.

Thickness of projection: B, 5 μm; C, 7 μm D, 9.9 μm; E, 4 μm.

Scale bars = 100 μm in A,C-E, 50 μm in B.

C, cumulus; Cb, cell body; Gs, ordinary glomeruli; T toroid

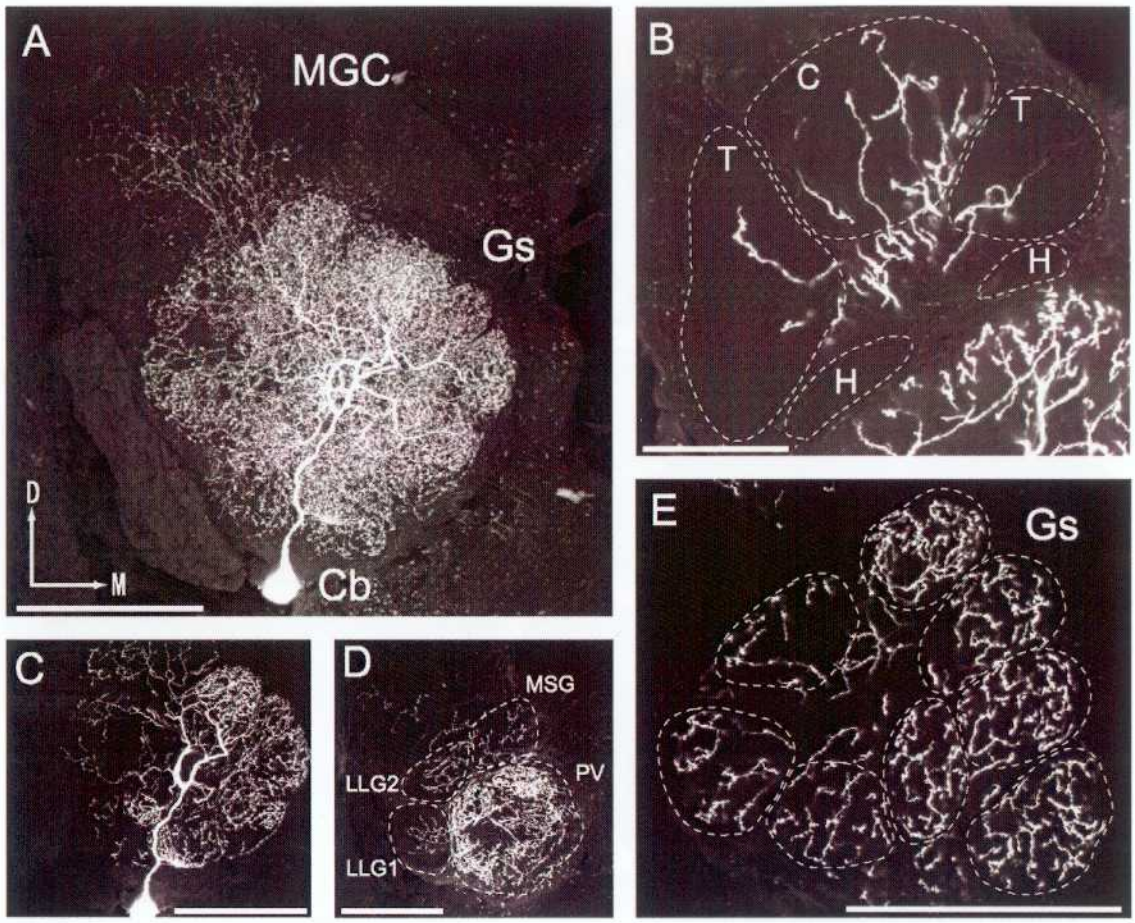
A
MGC
Gs
D
M
Cb
B
C
T
T
H
H
C
D
MSG
PV
LLG2
LLG1
E
Gs

Fig. 16

Type III LNs

A: Full structure of the Type IIIa LN. It arborizes in pluri-Gs. It has cell body in the LC I. It sends its main neurite to the center core of the AL and then radially branches. The boxes show the region magnified in B and C. **B, C**: Magnification view of dendritic branches. **D**: Full structure of the Type IIIb LN. It arborizes in pluri-Gs. It has large sized cell body (>20 μm) in the LC I. It sends its main neurite through posterior to the major tract and send its thick axons (6 μm at the thickest part) drawing arch like tract. The boxes are magnified in E and F. **E, F**: Magnification view of dendritic branches. **G, H**: Another examples of full structure of the Type IIIa LN. **I**: Another example of full structure of the Type IIIb LN.

Thickness of projection: B, 10.8 μm; C, 18 μm E, 14.7 μm; F, 14 μm.

Scale bars = 100 μm in A,D,G,H,I; 20 μm in B, C, E, F

Cb, cell body; Gs, ordinary glomeruli

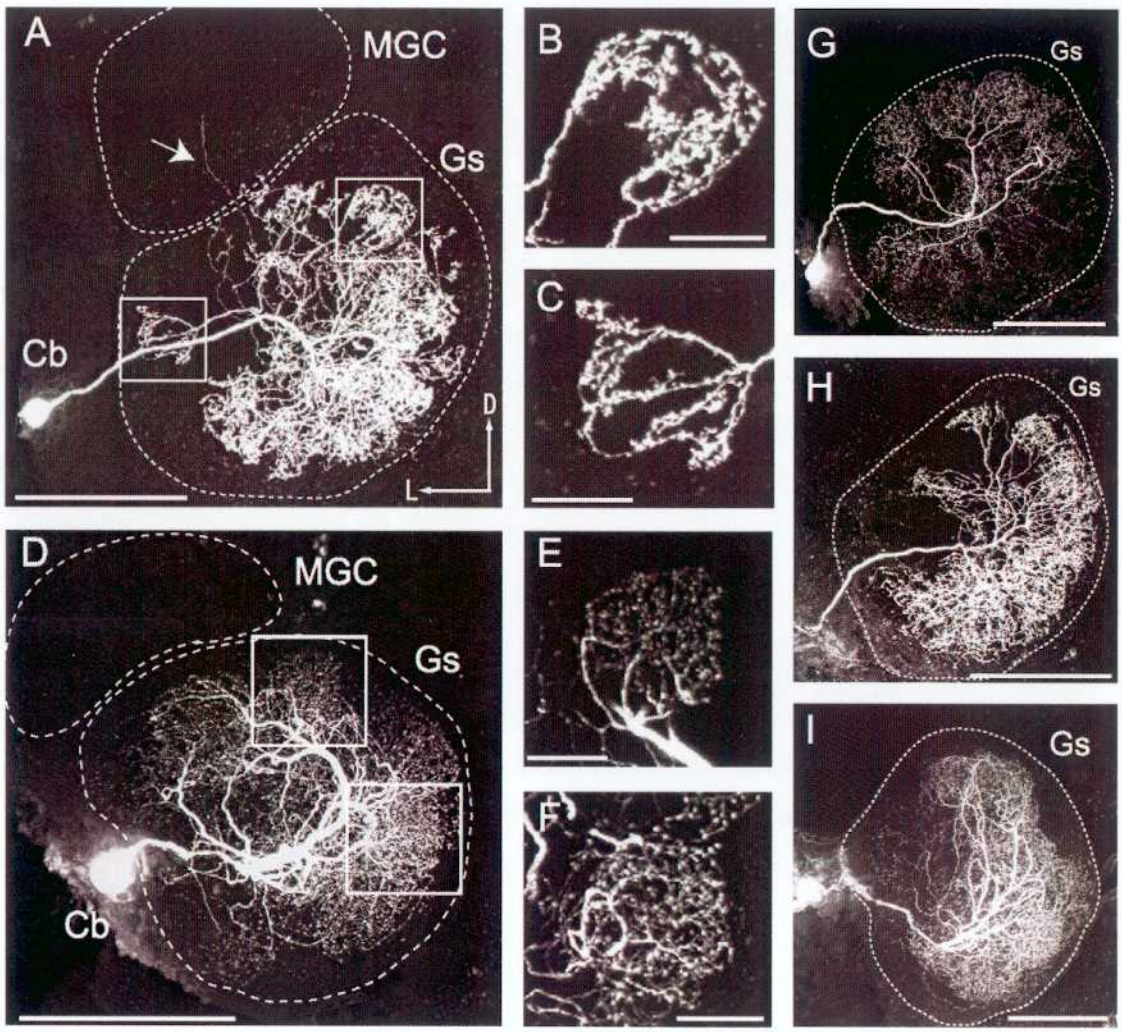
A
MGC
Gs
Cb
D
L
B
C
G
Gs
H
Gs
D
MGC
Gs
Cb
E
F
I
Gs

Fig. 17

Type IV LNs

A, B: Two example of full structure of the Type IVa LNs. It arborizes in the MGC and the pluri-Gs. It has cell body in the LC I. It sends its main neurite to the center core of the AL. Branches in the Gs region are biased to the upper region under the MGC. **C**: Full structure of the Type IVb LN. It arborizes in the MGC and the pluri-Gs. It has cell body in the LC I. It sends its main neurite to the center core of the AL and then send branches radially to the about 40% Gs. **D**: Full structure of the Type IVb LN. It arborizes in the MGC and the pluri-Gs. It has cell body in the LC I. It sends its main neurite to the center core of the AL through posterior to the major fiber tract. Branches in the Gs region are a few of the Gs under the MGC at the surface of Gs and the PV. **E**: Full structure of the Type IVc LN. It arborizes in the MGC, pluri-Gs and the AMMC. It has cell body in the LC I. It sends its main neurite to the center core of the AL through posterior to the major fiber tract. Branches at the center core of the AL are also observed. **F**: Projection image of several slices of the type IV LN arborizing in the AMMC.

Thickness of projection: E, 34 μm; F, 14 μm.

Scale bars = 100 μm.

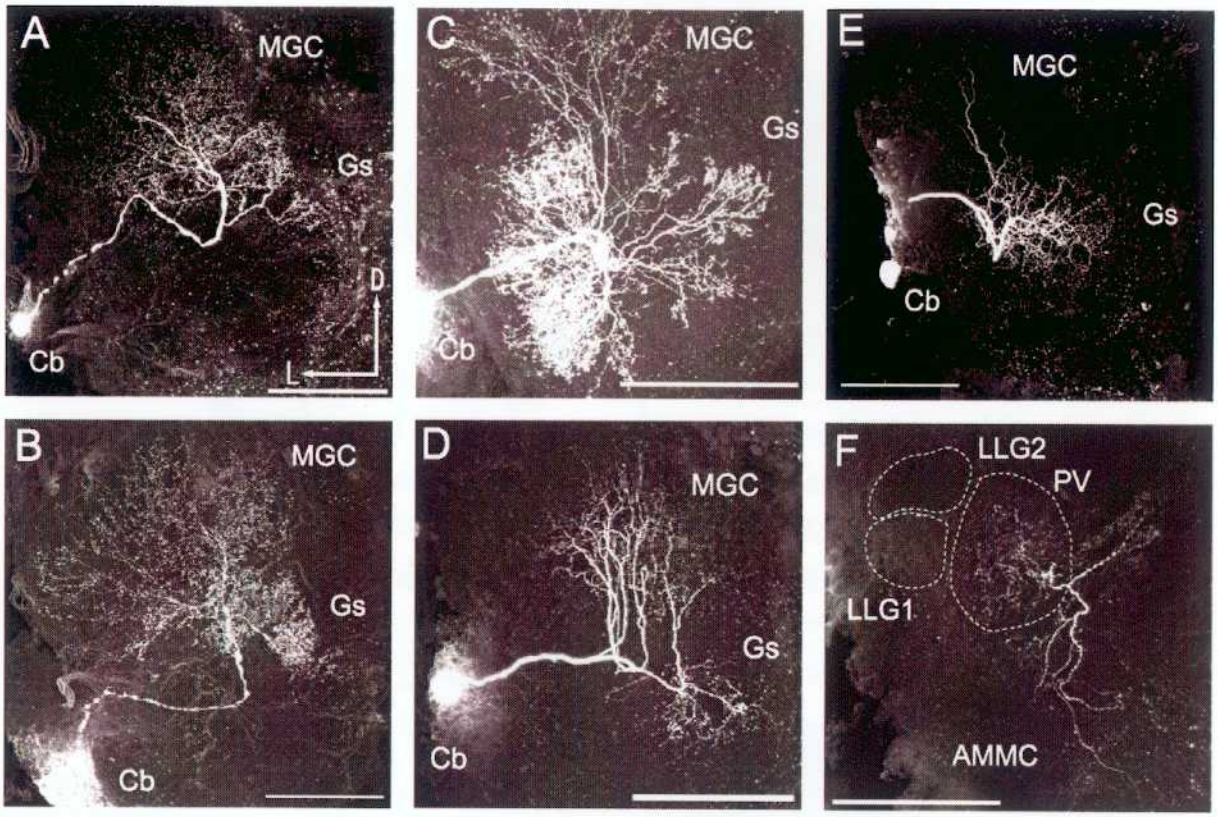
A
MGC
Gs
D
L
Cb
C
MGC
Gs
Cb
E
MGC
Gs
Cb
B
MGC
Gs
Cb
D
MGC
Gs
Cb
F
LLG2
PV
LLG1
AMMC

Fig. 18

Distribution of cell bodies of the LNs in the LC

I define the one LC which seems to have the average shape as a standard. I plot the position of the cell bodies of LNs on the standard LC. To the vertical direction the LC is divided into four layers by 30 μm. Approximate positions of the cell bodies are plotted two dimensionally in the standard LC. Cell body size is roughly expressed as larger size for the type II LNs and type IIIb LNs than the other type LNs.

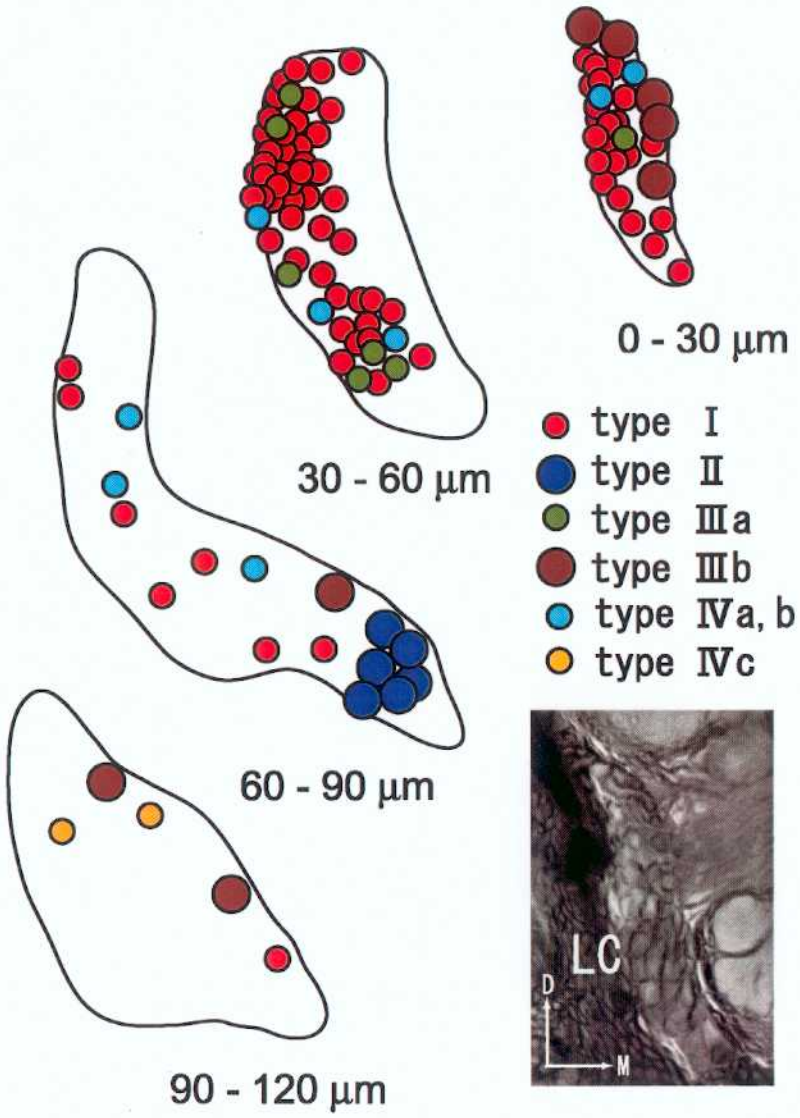
0 - 30 μm
30 - 60 μm
60 - 90 μm
90 - 120 μm
type I
type II
type IIIa
type IIIb
type IVa, b
type IVc
LC
D
M

Fig.19

Double labeling of ORNs-LN (A-C) and LN-PN (D,E).

A-C: Projection image of a few slices of the LY stained LN (green) and the TMR stained ORNs (red). Schematic diagram is shown left. The boxes are magnified in B and C. **D, E**: Projection image of a few slices of the Alexa flour 568 stained LN and the LY stained uniglomerular PNs. The box is magnified in E. Schematic diagram is shown left. Thickness of projection: A-E, 5.6 μm.

Scale bars = 100 μm in A,D; 20 μm in B,C,E.

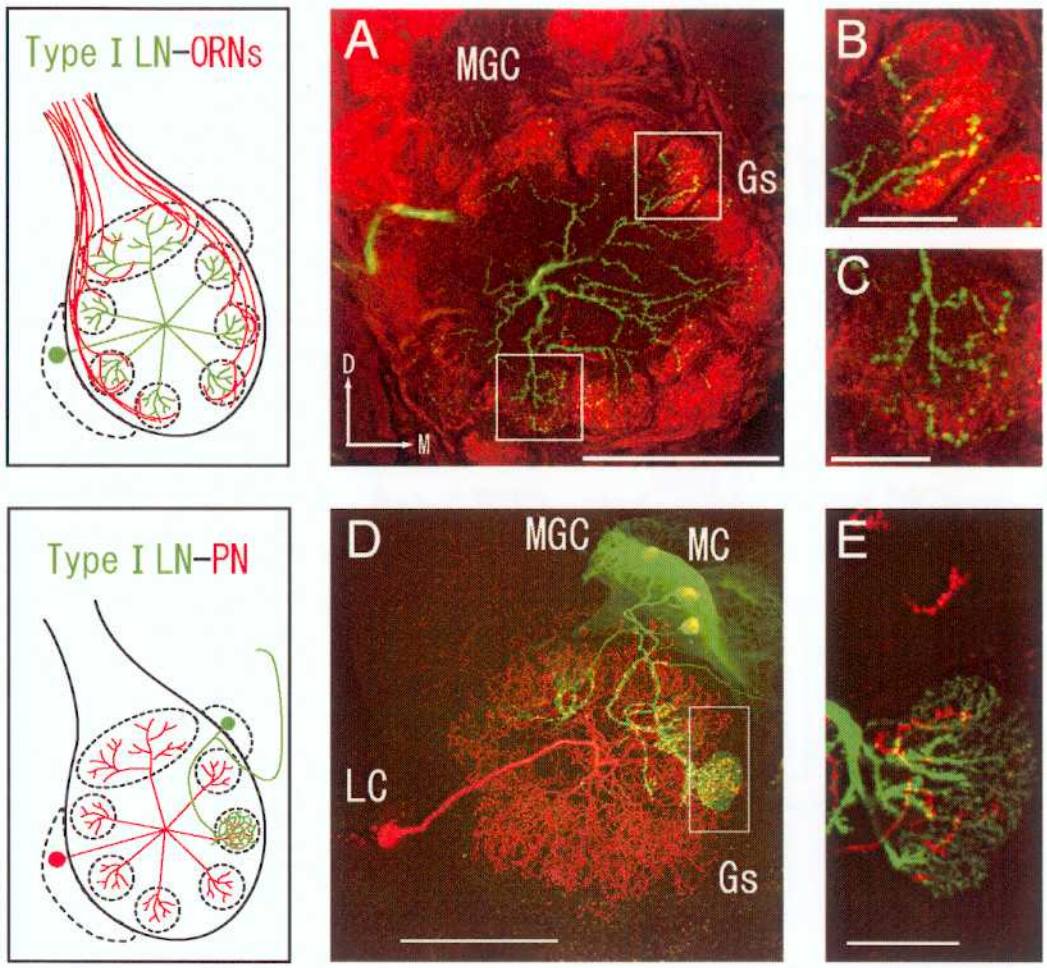
Type I LN-ORNs
A
MGC
Gs
D
M
B
C
Type I LN-PN
D
MGC
MC
LC
Gs
E

Fig. 20

Schematic diagram of the projection paths of PNs from subdivisions of the MGC and the ordinary glomerulus to the LPC. Toroid-PNs project their axon to the whole ΔILPC (red). Cumulus- and horseshoe-PNs project their axon to the lateral half of the ΔILPC (blue). G-PNs project to the LH (green). Reanalysis of our previous result demonstrated the possibility that c+t-PNs which have dendritic arborizations in the cumulus and toroid project their axon to the lateral half of the ΔILPC by passing the Ca (dotted black line). See text for detail.

Ca, calyx of the mushroom body; ΔILPC, delta area in the inferior lateral protocerebrum; G, ordinary glomerulus; IACT, inner antenno-cerebral tract; MACT middle antenno-cerebral tract; MGC, macroglomerular complex; OACT, outer antenno-cerebral tract

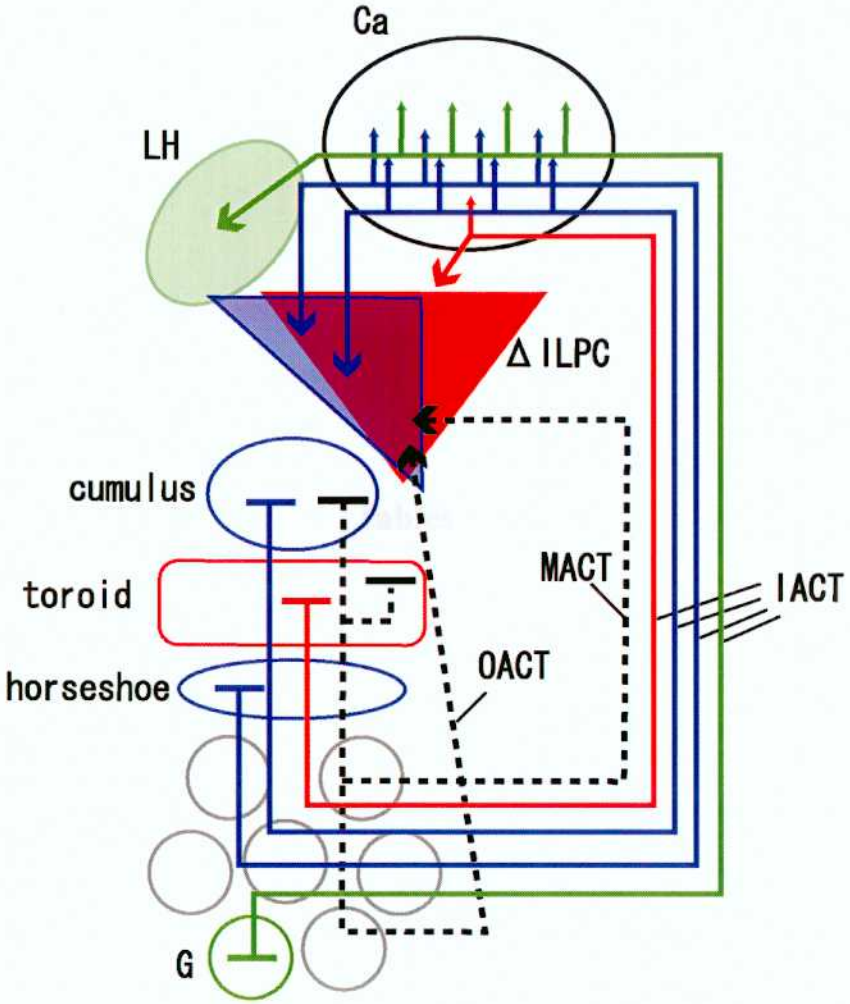
Ca
LH
ΔILPC
cumulus
toroid
horseshoe
MACT
IACT
OACT
G